GSA Data repository item 2018128

Strontium and carbon isotopic evidence for decoupling of pCO_2 from continental weathering at the apex of the late Paleozoic glaciation

Jitao Chen[1,2,3*], Isabel P. Montañez[1], Yuping Qi[2,3], Shuzhong Shen[2,4], and Xiangdong Wang[2,3]

[1]*Department of Earth and Planetary Sciences, University of California-Davis, Davis, California 95616, USA*
[2]*Center for Excellence in Life and Paleoenvironment, Chinese Academy of Sciences, Nanjing 210008, China*
[3]*CAS Key Laboratory of Economic Stratigraphy and Palaeogeography, Nanjing Institute of Geology and Palaeontology, Chinese Academy of Sciences, Nanjing 210008, China*
[4]*State Key Laboratory of Palaeobiology and Stratigraphy, Nanjing Institute of Geology and Palaeontology, Chinese Academy of Sciences, Nanjing 210008, China*
*E-mail: jtchen@nigpas.ac.cn

Sr Isotope Analysis

Conodonts (n=99) recovered from the ~280-m-thick Naqing carbonate succession were ultrasonicated for ~10–20 seconds to remove possible attached silicate minerals (Ebneth et al., 1997) and leached in 0.5% acetic acid for 12–16 hours to remove the diagenetically more susceptible outer layer (Ruppel et al., 1996). Conodont elements were subsequently dissolved in 3 N Optima© nitric acid for column chemistry. Carbonate samples (n=22) were thin-sectioned and stained with Alizarin Red-S and Potassium Ferricyanide. Target areas for microsampling and analysis (i.e., well-preserved micrite) were identified using transmitted and cathodoluminescent microscopy. Pink-staining (i.e., low [Fe^{2+}]), non/dully luminescent micrite was microdrilled from thick sections (70–100 μm thick). Drilled powders (2–3 mg) were prewashed three times with 0.2 N ammonium acetate solution and rinsed repeatedly in nanopure water in order to remove adsorbed or exchangeable Sr from non-carbonate phases (Montañez et al., 2000). Prewashed samples were dissolved in 4% Optima© acetic acid, dried down, and dissolved in 3 N Optima© nitric acid for column chemistry.

Age Calibration for Data Sets

Ages for conodont and carbonate $^{87}Sr/^{86}Sr$ (this study) and previously published carbonate $\delta^{13}C$ (Buggisch et al., 2011) of the Naqing section were calibrated using the Carboniferous (Davydov et al., 2012) and Permian time scales (Henderson, 2016) and our updated conodont biostratigraphy (Fig. 1; Qi et al., 2014, 2016, and unpublished data),

assuming constant sedimentation rate within stages. Visean data ages (middle Mississippian) were calculated assuming the same sedimentation rate as the overlying Serpukhovian stage. The ages of previously published data presented in Figure 2 were also normalized to the geological time scales used in this paper.

Revision of pCO_2 values for Montañez et al. (2007)

The older subset of the latest Carboniferous through early Permian pCO_2 values first presented in Montañez et al. (2007) were revised using PBUQ of Breecker (2013) and presented in a recent paper (Montañez et al., 2016). The remaining pCO_2 values of Montañez et al. (2007) have been revised using soil-specific soil-respired CO_2 (Sz) values of Montañez (2013; unpublished data; squares in Fig. 2D).

References Cited

Breecker, D.O., 2013, Quantifying and understanding the uncertainty of atmospheric CO_2 concentrations determined from calcic paleosols: Geochemistry, Geophysics, Geosystems, v. 14, p. 3210–3220, doi: 10.1002/ggge.20189.

Buggisch, W., Wang, X., Alekseev, A.S., and Joachimski, M.M., 2011, Carboniferous–Permian carbon isotope stratigraphy of successions from China (Yangtze platform), USA (Kansas) and Russia (Moscow Basin and Urals): Palaeogeography, Palaeoclimatology, Palaeoecology, v. 301, p. 18–38, doi: 10.1016/j.palaeo.2010.12.015.

Davydov, V.I., Korn, D., and Schmitz, M.D., 2012, The Carboniferous Period, *in* Gradstein, F., Ogg, J., Schmitz, M., and Ogg, G., eds., The Geologic Time Scale 2012: London, Elsevier, p. 615–663, doi: 10.1016/B978-0-444-59425-9.00023-8.

Ebneth, S., Diener, A., Buhl, D., and Veizer, J., 1997, Strontium isotope systematics of conodonts: Middle Devonian, Eifel Mountains, Germany: Palaeogeography Palaeoclimatology Palaeoecology, v. 132, p. 79–96, doi: org/10.1016/S0031-0182(97)00057-6.

Henderson, C.M., 2016, Permian conodont biostratigraphy, *in* Lucas, S.G., and Shen, S.Z., eds., The Permian Timescale: London, Geological Society Special Publications, in press, doi: 10.1144/sp450.9.

Montañez, I.P., 2013, Modern soil system constraints on reconstructing deep-time atmospheric CO_2: Geochimica et Cosmochimica Acta, v. 101, p. 57–75, doi: 10.1016/j.gca.2012.10.012.

Montañez, I.P., Osleger, D.A., Banner, J.L., Mack, L.E., and Musgrove, M., 2000, Evolution of the Sr and C isotope composition of Cambrian oceans: GSA Today, v. 10, p. 1–7.

Montañez, I.P., McElwain, J.C., Poulsen, C.J., White, J.D., DiMichele, W.A., Wilson, J.P., Griggs, G., and Hren, M.T., 2016, Climate, pCO_2 and terrestrial carbon cycle linkages during late Palaeozoic glacial–interglacial cycles: Nature Geoscience, v. 9, p. 824–828, doi: 10.1038/ngeo2822.

Qi, Y.-P., Lambert, L.L., Nemyrovska, T.I., Wang, X.-D., Hu, K.-Y., and Wang, Q.-L., 2016, Late Bashkirian and early Moscovian conodonts from the Naqing section, Luodian, Guizhou, South China: Palaeoworld, v. 25, p. 170–187, doi: 10.1016/j.palwor.2015.02.005.

Qi, Y., Nemyrovska, T.I., Wang, X., Chen, J., Wang, Z., Lane, H.R., Richards, B.C., Hu, K., and Wang, Q., 2014, Late Visean–early Serpukhovian conodont succession at the Naqing (Nashui) section in Guizhou, South China: Geological Magazine, v. 151, p. 254–268, doi: 10.1017/S001675681300071X.

Ruppel, S.C., James, E.W., Barrick, J.E., Nowlan, G., and Uyeno, T.T., 1996, High-resolution $^{87}Sr/^{86}Sr$ chemostratigraphy of the Silurian: Implications for event correlation and strontium flux: Geology, v. 24, p. 831–834, doi: 10.1130/0091-7613(1996)024<0831:HRSSCO>2.3.CO;2.

Supplementary Figures

Figure DR1. Late Carboniferous paleogeography (courtesy of R. Blakey) showing locations of the Naqing section (25°14′40″N, 106°29′26″E), south China, and seawater $^{87}Sr/^{86}Sr$ and $\delta^{13}C$ records referred to in this study. 1—Midcontinent, USA; 2—Moscow Basin, Russia; 3—Urals, Russia; 4—Donets Basin, Ukraine; 5—Akiyoshi terrane, Japan.

Figure DR2. Comparison of original values and LOESS results of the conodont based $^{87}Sr/^{86}Sr$ (this study and Henderson et al., 2012) using 0.1, 0.2, and 0.3 smoothing parameter. The inflexion in the $^{87}Sr/^{86}Sr$ curve from rising to plateau is determined by the abrupt change in $^{87}Sr/^{86}Sr$ values from 0.808193 at 317.78 Ma to 0.708223 at 317.62 Ma (Table DR1), which is also supported by a change in rising rate of $^{87}Sr/^{86}Sr$ before and after 317.78–317.62 Ma based on the LOESS results. The inflexion in the $^{87}Sr/^{86}Sr$ curve from plateau to falling is determined by the abrupt change in $^{87}Sr/^{86}Sr$ value from 0.708321 at 303.81 Ma to 0.708279 at 302.8 Ma, which is supported by the abrupt change in $^{87}Sr/^{86}Sr$ from nearly constant to rapidly declining based on the LOESS results.

Supplementary Tables

Table DR1. Conodont $^{87}Sr/^{86}Sr$ from the Naqing section, south China
Table DR2. Carbonate $^{87}Sr/^{86}Sr$ from the Naqing section, south China

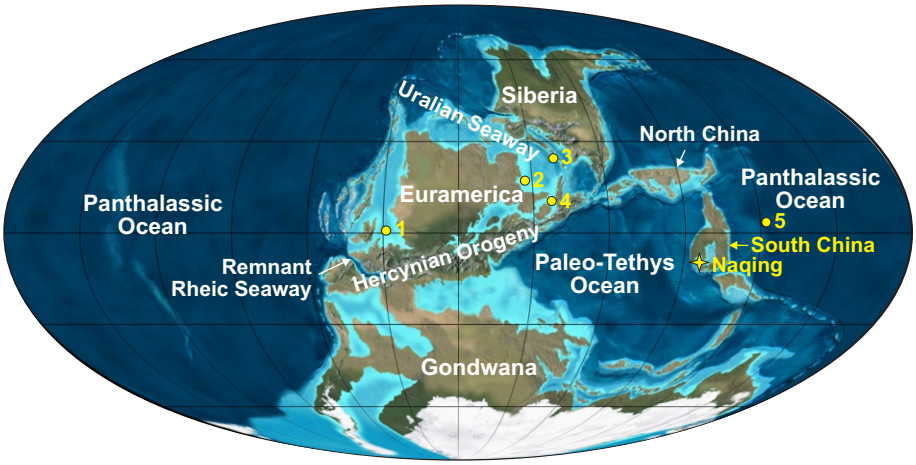

Figure DR1. Late Carboniferous paleogeography (courtesy of R. Blakey) showing locations of the Naqing section (25°14′40″N, 106°29′26″E), south China, and seawater $^{87}Sr/^{86}Sr$ and $\delta^{13}C$ records referred to in this study. 1—Midcontinent, USA; 2—Moscow Basin, Russia; 3—Urals, Russia; 4—Donets Basin, Ukraine; 5—Akiyoshi terrane, Japan.

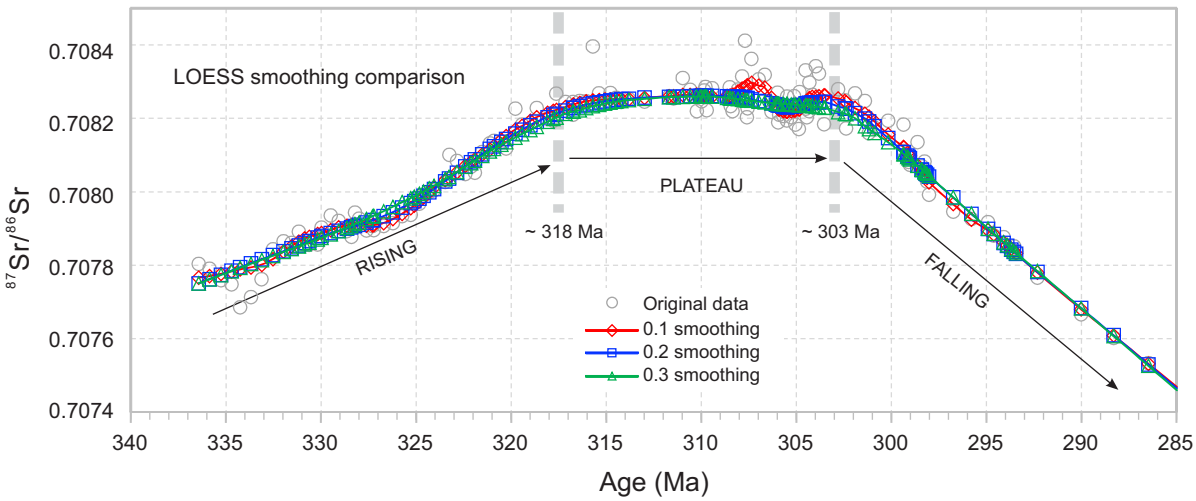

Figure DR2. Comparison of original values and LOESS results of the conodont based $^{87}Sr/^{86}Sr$ (this study and Henderson et al., 2012) using 0.1, 0.2, and 0.3 smoothing parameter. The inflexion in the $^{87}Sr/^{86}Sr$ curve from rising to plateau is determined by the abrupt change in $^{87}Sr/^{86}Sr$ values from 0.808193 at 317.78 Ma to 0.708223 at 317.62 Ma (Table DR1), which is also supported by a change in rising rate of $^{87}Sr/^{86}Sr$ before and after 317.78–317.62 Ma based on the LOESS results. The inflexion in the $^{87}Sr/^{86}Sr$ curve from plateau to falling is determined by the abrupt change in $^{87}Sr/^{86}Sr$ value from 0.708321 at 303.81 Ma to 0.708279 at 302.8 Ma, which is supported by the abrupt change in $^{87}Sr/^{86}Sr$ from nearly constant to rapidly declining based on the LOESS results.

Table DR1: Conodont based 87Sr/86Sr from Naqing section, south China

	Sample number	Meter above the base (m)	87Sr/86Sr	2SE	Age (Ma)	Stage
1	NC 10	10.00	0.707803	0.000010	336.44	Visean
2	LDC 15.3	15.30	0.707791	0.000012	335.86	Visean
3	LDC 20.7	20.70	0.707759	0.000012	335.26	Visean
4	LDC 25.7	25.70	0.707748	0.000014	334.71	Visean
5	LDC 29.8	29.80	0.707685	0.000013	334.25	Visean
6	LDC 35	35.00	0.707713	0.000011	333.68	Visean
7	LDC 40	40.00	0.707761	0.000013	333.12	Visean
8	NSC 45.4	45.40	0.707843	0.000014	332.53	Visean
9	NSC 50.4	50.40	0.707865	0.000010	331.97	Visean
10	NSC 54.25	54.25	0.707860	0.000020	331.55	Visean
11	NSC 57.7	57.70	0.707891	0.000019	331.17	Visean
12	LDC 60.48	60.48	0.707857	0.000015	330.86	Serpukhovian
13	NSC 62.6	62.60	0.707856	0.000023	330.62	Serpukhovian
14	NSC 66.6	66.60	0.707856	0.000016	330.18	Serpukhovian
15	NSC 68.5	68.50	0.707902	0.000013	329.97	Serpukhovian
16	LDC 72.88	72.88	0.707936	0.000013	329.49	Serpukhovian
17	LDC 76.65	76.65	0.707920	0.000010	329.07	Serpukhovian
18	LDC 80.55	80.55	0.707893	0.000010	328.64	Serpukhovian
19	LDC 82.65	82.65	0.707877	0.000013	328.41	Serpukhovian
20	LDC 84.4	84.40	0.707943	0.000013	328.21	Serpukhovian
21	LDC 86.4	86.40	0.707927	0.000011	327.99	Serpukhovian
22	LDC 89.85	89.85	0.707895	0.000012	327.61	Serpukhovian
23	NC 92.75	92.75	0.707906	0.000010	327.29	Serpukhovian
24	LDC 93.3	93.30	0.707895	0.000011	327.23	Serpukhovian
25	LDC 98	98.00	0.707906	0.000012	326.71	Serpukhovian
26	LDC 102.42	102.42	0.707914	0.000012	326.22	Serpukhovian
27	LDC 106.8	106.80	0.707934	0.000013	325.73	Serpukhovian
28	LDC 110.9	110.90	0.707937	0.000013	325.28	Serpukhovian
29	LDC 112.6	112.60	0.707977	0.000009	325.09	Serpukhovian
30	LDC 115	115.00	0.707967	0.000013	324.83	Serpukhovian
31	LDC 117	117.00	0.707988	0.000011	324.61	Serpukhovian
32	LDC 119.7	119.70	0.707999	0.000011	324.31	Serpukhovian
33	LDC 122	122.00	0.708004	0.000016	324.05	Serpukhovian
34	LDC 127.25	127.25	0.708027	0.000010	323.47	Serpukhovian
35	LDC 129.2	129.20	0.708101	0.000010	323.26	Serpukhovian
36	LDC 131.7	131.70	0.708084	0.000010	322.85	Bashkirian
37	LDC 134.25	134.25	0.708048	0.000011	322.41	Bashkirian
38	LDC 136	136.00	0.708068	0.000012	322.11	Bashkirian
39	LDC 137.2	137.20	0.708052	0.000016	321.90	Bashkirian

40	LDC 139.4	139.40	0.708108	0.000012	321.52	Bashkirian
41	LDC 141.7	141.70	0.708132	0.000011	321.12	Bashkirian
42	LDC 143	143.00	0.708138	0.000013	320.90	Bashkirian
43	LDC 145.2	145.20	0.708136	0.000012	320.52	Bashkirian
44	LDC 146.7	146.70	0.708117	0.000007	320.26	Bashkirian
45	LDC 149.45	149.45	0.708226	0.000012	319.78	Bashkirian
46	L 151.5	151.50	0.708183	0.000012	319.43	Bashkirian
47	L 154	154.00	0.708187	0.000010	318.99	Bashkirian
48	NSC 156	156.00	0.708228	0.000011	318.65	Bashkirian
49	NSC 159.2	159.20	0.708199	0.000009	318.09	Bashkirian
50	NC161	161.00	0.708193	0.000012	317.78	Bashkirian
51	NSC 161.9	161.90	0.708267	0.000009	317.62	Bashkirian
52	NSC 164.7	164.70	0.708244	0.000010	317.14	Bashkirian
53	NC 167	167.00	0.708210	0.000010	316.74	Bashkirian
54	NSC 167.05	167.05	0.708245	0.000011	316.73	Bashkirian
55	NSC 169.05	169.05	0.708247	0.000012	316.39	Bashkirian
56	NSC 171	171.00	0.708247	0.000013	316.05	Bashkirian
57	LD 173	173.00	0.708396	0.000011	315.70	Bashkirian
58	LDC 174.9	174.90	0.708268	0.000010	315.37	Bashkirian
59	LDC 176.9	176.90	0.708239	0.000011	315.06	Moscovian
60	LDC 179.05	179.05	0.708269	0.000013	314.77	Moscovian
61	LDC 181.18	181.18	0.708256	0.000013	314.48	Moscovian
62	LD 183.2	183.20	0.708244	0.000011	314.20	Moscovian
63	LDC 186.14	186.14	0.708252	0.000011	313.80	Moscovian
64	NC 192.2	192.20	0.708246	0.000012	312.98	Moscovian
65	NC 201.6	201.60	0.708259	0.000011	311.69	Moscovian
66	LDC 203.4	203.40	0.708254	0.000010	311.45	Moscovian
67	LDC 206.9	206.90	0.708310	0.000009	310.97	Moscovian
68	NSC 209.7	209.70	0.708278	0.000009	310.59	Moscovian
69	NSC 213.5	213.50	0.708260	0.000009	310.07	Moscovian
70	NC 215.2	215.20	0.708276	0.000012	309.84	Moscovian
71	NSC 215.7	215.70	0.708286	0.000009	309.77	Moscovian
72	NSC 218.2	218.20	0.708282	0.000010	309.43	Moscovian
73	LDC 224	224.00	0.708256	0.000012	308.64	Moscovian
74	LDC 225	225.00	0.708284	0.000012	308.50	Moscovian
75	LDC 228.15	228.15	0.708278	0.000011	308.07	Moscovian
76	LDC 229.8	229.80	0.708314	0.000010	307.85	Moscovian
77	NSC 230.9	230.90	0.708411	0.000011	307.70	Moscovian
78	LDC 233.4	233.40	0.708362	0.000012	307.35	Moscovian
79	LDC 236.1	236.10	0.708306	0.000011	306.98	Kasimovian
80	LDC 238	238.00	0.708319	0.000009	306.66	Kasimovian
81	LDC 242	242.00	0.708270	0.000013	305.99	Kasimovian

82	LDC 245	245.00	0.708259	0.000011	305.49	Kasimovian
83	NSC 247.2	247.20	0.708260	0.000011	305.12	Kasimovian
84	LDC 248.95	248.95	0.708272	0.000011	304.83	Kasimovian
85	LDC 250.83	250.83	0.708331	0.000009	304.51	Kasimovian
86	LDC 252	252.00	0.708297	0.000015	304.31	Kasimovian
87	LDC 253	253.00	0.708264	0.000009	304.15	Kasimovian
88	LDC 254	254.00	0.708342	0.000010	303.98	Kasimovian
89	NSC 255	255.00	0.708321	0.000010	303.81	Kasimovian
90	LDC 256.9	256.90	0.708246	0.000009	303.48	Gzhelian
91	NSC 260.8	260.80	0.708279	0.000009	302.80	Gzhelian
92	NSC 262.75	262.75	0.708249	0.000015	302.45	Gzhelian
93	NSC 265.85	265.85	0.708268	0.000009	301.91	Gzhelian
94	LDC 268.8	268.80	0.708247	0.000011	301.39	Gzhelian
95	LDC 271.7	271.70	0.708174	0.000011	300.88	Gzhelian
96	LDC 275.8	275.80	0.708193	0.000014	300.16	Gzhelian
97	LDC 280.4	280.40	0.708183	0.000012	299.36	Gzhelian
98	L 284.6	284.60	0.708135	0.000010	298.62	Asselian
99	L 286.7	286.70	0.708082	0.000010	298.25	Asselian

Table DR2: Bulk carbonate 87Sr/86Sr from Naqing section, south China

	Sample number	Meter above the base (m)	Sr87/86Sr	2SE	Age (Ma)	Stage
1	NQi 51.2	51.20	0.708041	0.000021	331.88	Visean
2	NQi 54.2	54.20	0.707953	0.000023	331.55	Visean
3	NQi 60.5	60.50	0.708130	0.000018	330.86	Serpukhovian
4	NQi 62.5	62.50	0.708048	0.000017	330.63	Serpukhovian
5	NQi 64.5	64.50	0.708131	0.000024	330.41	Serpukhovian
6	NQi 68.5	68.50	0.708055	0.000022	329.97	Serpukhovian
7	NQi 115.05	115.05	0.708263	0.000022	324.82	Serpukhovian
8	NQi 117.05	117.05	0.708263	0.000017	324.60	Serpukhovian
9	NQi 119.22	119.22	0.708288	0.000020	324.36	Serpukhovian
10	NQi 120.8	120.80	0.708265	0.000018	324.18	Serpukhovian
11	NQi 122.21	122.21	0.708144	0.000022	324.03	Serpukhovian
12	NQi 126.4	126.40	0.708149	0.000019	323.57	Serpukhovian
13	NQi 128.35	128.35	0.708192	0.000023	323.35	Serpukhovian
14	NQi 129.35	129.35	0.708264	0.000021	323.24	Serpukhovian
15	NQi 130.45	130.45	0.708217	0.000015	323.07	Bashkirian
16	NQi 131.45	131.45	0.708154	0.000021	322.90	Bashkirian
17	NQi 133.35	133.35	0.708158	0.000023	322.57	Bashkirian
18	NQi 135.55	135.55	0.708216	0.000024	322.19	Bashkirian
19	NQi 137	137.00	0.708200	0.000022	321.94	Bashkirian
20	NQi 141.1	141.10	0.708344	0.000018	321.23	Bashkirian
21	NQi 145.36	145.36	0.708371	0.000018	320.49	Bashkirian
22	NQi 147.2	147.20	0.708355	0.000017	320.17	Bashkirian